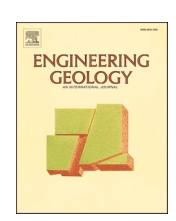
ELSEVIER

Contents lists available at ScienceDirect

Engineering Geology

journal homepage: www.elsevier.com/locate/enggeo



Check for updates

Impact of hysteresis of unsaturated hydraulic properties on rainfall-induced slope failures

Levinna Natalia, Jun Yang

Department of Civil Engineering, The University of Hong Kong, Hong Kong, China

ARTICLE INFO

Keywords:
Rainfall-induced landslides
Soil-water characteristic curve
Hysteresis
Landslide hazard
Parameter selection

ABSTRACT

The devastating consequences of rainfall-induced slope failures call for considering more realistic scenarios in slope engineering. As the matric suction in unsaturated soil varies with climatic conditions, hysteresis behavior is observed in the drying (desorption) and wetting (adsorption) processes. The soil water characteristic curve (SWCC) is essential in describing the relationship between the water content and matric suction. Previous studies contained diverging views on selecting SWCC for slope stability analysis, particularly concerning the hysteresis behavior. Here we present an investigation into the impact of hysteresis in SWCC on the stability of unsaturated soil slopes. Different SWCC shapes, designed to compare the influence of selecting drying and wetting curves on rainfall-induced landslides under various rainfall characteristics, permeability, and initial suction, are examined. We observe that the SWCC resembling the characteristic of the drying curve results in more critical conditions and more significant fluctuations in safety factor when subjected to rainfall and no-rainfall events. The magnitude of initial suction relative to the air-entry value potentially explains the diverging views in the literature of whether the drying or wetting curve ensures a safer slope stability analysis. The findings from this study have significant implications for slope stability evaluation, particularly emphasizing the importance of considering hysteresis, heterogeneity, parameter uncertainty in design.

1. Introduction

Rainfall-induced slope failure has been an issue due to its damaging consequences. Climate change and increase in land use increase land-slide susceptibility around the world (Ho et al., 2016; Kim et al., 2021; Yang et al., 2022), adding to the urgency to mitigate these devastating events. Numerous attempts have been made to understand the controlling factors, failure mechanisms, and prevention of these instabilities. Previous studies observed that the hydrological mechanisms for rainfall-induced slope failures involve either (1) the rising of the water table or (2) the dissipation of matric suction and possible development of positive porewater pressure. Previous observations found that only 2 % of slope failures in Hong Kong were attributed to rising groundwater levels (Wong and Ho, 1993).

The porewater pressure development has been identified as one of the factors reducing the soil strength. In the case of contractive soil, it might potentially cause strain-softening or collapse behavior and subsequently cause flowslides, which have rapid velocity and extreme runout distance (Wang and Sassa, 2003; Yang and Wei, 2012). The

phenomenon has been observed in previous studies related to rainfall-induced slope failures under both drained and undrained scenarios (Anderson and Sitar, 1995; Chen and Yang, 2024; Wang and Sassa, 2003; Zhang et al., 2023; Zou et al., 2024). In this regard, it is of practical interest to quantify the amount of water infiltrating the soil and understand how it might influence slope stability.

The soil water characteristic curve (SWCC) represents the relationship between suction and the amount of water in a soil, which can be represented using either gravimetric water content, volumetric water content, or degree of saturation. Studies showed that the relationship between the suction and the water content in the soil differs, as shown in Fig. 1, depends on the process experienced by the soil - whether it is drying or wetting. This phenomenon is known as hysteresis. The hysteresis phenomena have been observed through laboratory experiments (Kim et al., 2018; Pang, 1999; Yang et al., 2004) and field measurements (Ni, 2017; Torres et al., 1998). The hysteresis of the soil is closely related to the grain-size distribution and dry density of the soil (Gallage and Uchimura, 2010; Yang et al., 2004). Previous studies have proposed different mechanisms explaining the phenomena (Hillel, 2003):

E-mail addresses: blevnatl@hku.hk (L. Natalia), junyang@hku.hk (J. Yang).

^{*} Corresponding author.

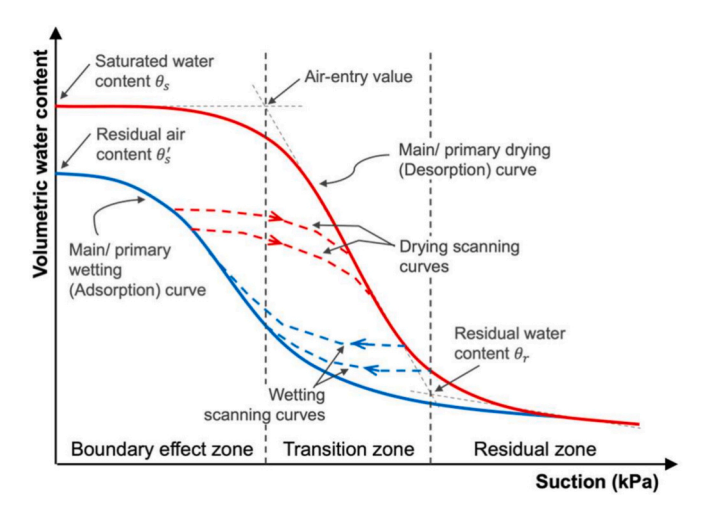


Fig. 1. Hysteresis in SWCC (after Fredlund et al., 1994; Zhai et al., 2020).

- The irregularity in the cross-section of the voids results in different behavior when water flows in and out of the void, known as the capillary theory or the "ink bottle effect."
- 2. The shrinkage and swelling caused by cycles of drying and wetting in a soil mass might cause changes in the soil fabric, structure, and pore size distribution.
- 3. The influence of the contact angle between air-water and soil solids being greater in advancing meniscus (wetting) than in a receding meniscus (drying).
- 4. The difference in the volume of entrapped air when the soil suction increases and decreases.

The drying and wetting curves starting from saturation are commonly referred to as main/ primary drying and wetting curves, respectively. The main drying and wetting curves enclose the hysteresis region, and families of drying and wetting scanning curves can exist between the main drying and wetting SWCC, as shown in Fig. 1. The scanning curves are a series of SWCC that start from a particular condition between saturated and dry. Depending on the antecedent and seepage condition experienced by the soil, the soil might experience a transition period when moving from the main drying to the main wetting curve (or vice versa). The process follows the path of scanning curves, which are observed to have relatively flatter gradients compared to the main curves, as shown in Fig. 1. However, for practical purposes, the main curves are more often adopted and received more attention in previous studies. Furthermore, due to various reasons such as practicality, resource limitations, and data availability, the analyses of slope instability induced by rainfall were usually performed using main drying SWCC (Li et al., 2013; Liu et al., 2020; Rianna et al., 2014; Zhang et al., 2016). One of the main reasons is that measuring the main wetting SWCC is a more time-consuming and costly task. Some studies provided alternative methods to predict the main wetting and scanning curves through mathematical equations using the main drying curve (Pham et al., 2005; Zhai et al., 2020). Nevertheless, the commonly used design software or methods usually only allow limited SWCC input in their analysis. Thus, the user's judgement is required to determine the most suitable SWCC for the analysis to be conducted.

Fig. 2 compares the laboratory and field SWCC of a Completely Decomposed Granite (CDG) slope in Ma On Shan, Hong Kong, measured at different depths and locations (Li, 2003). The field measured SWCC shows less apparent hysteresis than the SWCC measured from the laboratory using a conventional pressure-plate extractor. Additionally, significant variability between SWCC measured at various locations can be observed, which is explainable as the SWCC of soil can be influenced by various factors such as the stress state, soil structure, and initial compaction water content (Li and Vanapalli, 2022). As illustrated in

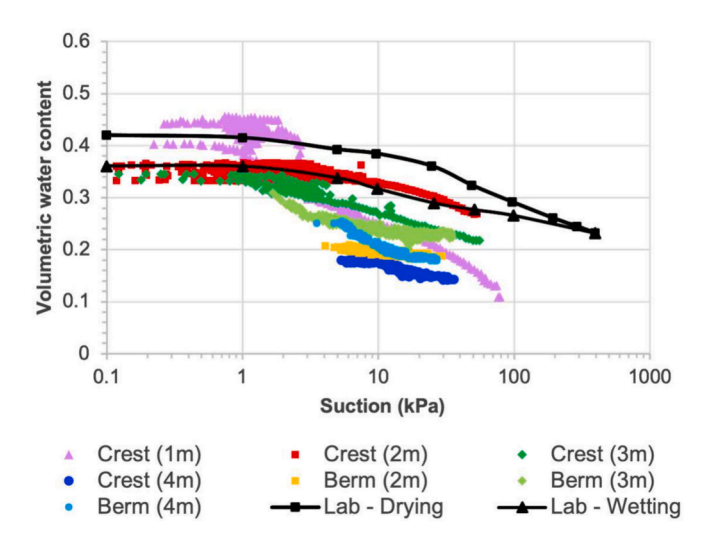


Fig. 2. Comparison of laboratory and field soil-water characteristic curves for CDG soil at different depths and locations within the same slope (after Li, 2003).

Fig. 1 and Fig. 2 (solid lines), the differences between drying and wetting SWCC could affect the accuracy of slope stability analysis against rainfall.

Some studies (Kristo et al., 2019; Zhai et al., 2016; Zhang, 2007) indicated that the drying curve, which is often adopted in practice, yields more conservative results in terms of slope stability. Several other studies, however, considered wetting curves for rainfall-induced instability analysis to be more appropriate as the soil undergoes the wetting process and the results are more conservative (Ebel et al., 2010; Kim et al., 2018; Tsai, 2011). Moreover, Tami et al. (2004) argued that the appropriate hydraulic properties of soil (i.e., drying or wetting) should be used according to the process that the soil experiences. These diverging views indicate the complexity of the problem and the need for further study to explore the possible reason for the divided opinions.

Adding to the complication, rainfall characteristics and soil heterogeneity are strongly related to the seepage profile and influence the landslide susceptibility (Ering and Babu, 2016; Ko and Lo, 2016; Yang et al., 2024). As illustrated in Fig. 2, inherent variability within the slope adds to the complexity of which SWCC should be adopted in the analysis. As rainfall-induced slope instability is an intricate process due to the interplays among various factors, a study with the aim to understand how SWCC selection influences failure mechanisms is worthwhile.

This study will first discuss the diverging views in previous studies related to the impact of SWCC selection on evaluating rainfall-induced slope stability. Through the literature review, the frameworks used in previous studies are compared, and two opposing views are examined in detail: whether the SWCC resembling the drying or wetting curve is the safer option for reliable design. A specifically designed parametric study is then carried out to explore the possible reason for the diverging views. Particularly, the impact of the SWCC shape on slope stability is evaluated across varying scenarios, such as rainfall characteristics, soil permeability, and the magnitude of initial suction. Additionally, SWCC measurements of typical soils in Hong Kong are collected, and their upper, average, and lower bounds are suggested for practical reference. The significant findings and the practical implications are also discussed.

2. Diverging views on unsaturated hydraulic properties related to slope instability

The influence of using drying and wetting SWCC on slope stability was studied by means of infiltration tests on a specially designed centrifuge to simulate field infiltration (Tami et al., 2004). The wetting

and drying processes were observed by having a lower and a higher ratio of antecedent rainfall to main rainfall intensity, respectively. The results were compared with numerical analysis using the measured SWCC and permeability function. The study concluded that appropriate hydraulic properties of soil, whether drying or wetting, should be based on the process experienced by the soil rather than the flux-boundary condition or the rainfall pattern. In the steady-state condition, they observed that although the soil was subjected to infiltration, it might experience a drying or wetting process depending on the antecedent conditions. Soil with higher antecedent conditions compared to the infiltration will experience a drying process as it discharges more water through evaporation and redistribution within the soil layer. Likewise, when the antecedent condition is lower than the infiltrating water, the soil will experience a wetting process. Subsequently, they observed that matric suction does not necessarily decrease during rainfall; rather, it depends on the process it experienced. However, the influence of these factors on slope stability was not investigated in that study.

While the conclusion found by Tami et al. (2004) is useful, most software programs in practice still only allow one SWCC as an input. Thus, when hysteresis is to be considered, the users must manually change the SWCC for different processes. This is not ideal, especially considering different drying and wetting processes can occur within soil layers. Additionally, the variability related to the influence of confining stress and density also contributes to the confusion of the parameter selection related to SWCC. Numerous studies have been conducted to determine which SWCC, wetting, drying, or the possibility of other alternatives, leads to more conservative results for rainfall-induced slope failures. However, the literature remains divided on whether to utilize drying or wetting SWCC for conservative design. A comprehensive study to explore the intricate interplays among various factors including rainfall characteristics will help to elucidate the diverging views and to advance our understating. This is exactly the motivation of this study.

Fig. 3 summarizes the SWCC utilized in the previous studies that are

considered in the following discussion. The upper and lower bound SWCC of residual soil in Singapore was estimated and found to be more suitable for estimating the permeability and unsaturated shear strength, respectively (Zhai et al., 2016). Additionally, when subjected to 1-day rainfall followed by a no-rainfall period, the upper bound SWCC, which resembles the drying curve relative to the wetting curve, produces the lowest factor of safety (FOS). Zhang (2007) compared the reliability of different scenarios: (1) only the drying curve, (2) the wetting curve for precipitation and drying curve for evaporation, and (3) averaging the wetting and drying curve. The first scenario is found to produce the lowest mean FOS. However, it has the highest coefficient of variation among the three scenarios, and thus, scores the lowest in terms of reliability index. Kristo et al. (2019) evaluated the influence of hysteresis on the stability of a residual soil slope (Bukit Timah Granite) in Singapore against various rainfall intensities. When subjected to cycles of rainfall and no-rainfall periods, the drying curve leads to a faster reduction and recovery of safety factors. They concluded that the wetting curve might be more reasonable for high-intensity rainfall, but overall, the drying SWCC gives more conservative results across rainfall intensity.

The influence of hysteresis on the hydro-mechanical behavior of unsaturated weathered granitic soil from Korea was investigated by using the Drucker-Prager criterion (Kim et al., 2018). They found that the main wetting SWCC results in the lowest soil strength and matric suction distribution. Similarly, Tsai (2011) and Ebel et al. (2010) utilized an infinite slope stability-based approach and concluded that drying SWCC will underestimate the potential failure of an unsaturated slope. Additionally, these studies observed that the SWCC influences not only the occurrence of slope instability but also the depth of slip surface, the time of failure, and the minimum landslide-triggering rainfall intensity and duration.

Evidently, the conclusions related to parameter selection of SWCC, especially when the hysteresis is considered in the rainfall-induced slope stability analysis, are still diverging. Some studies concluded that the

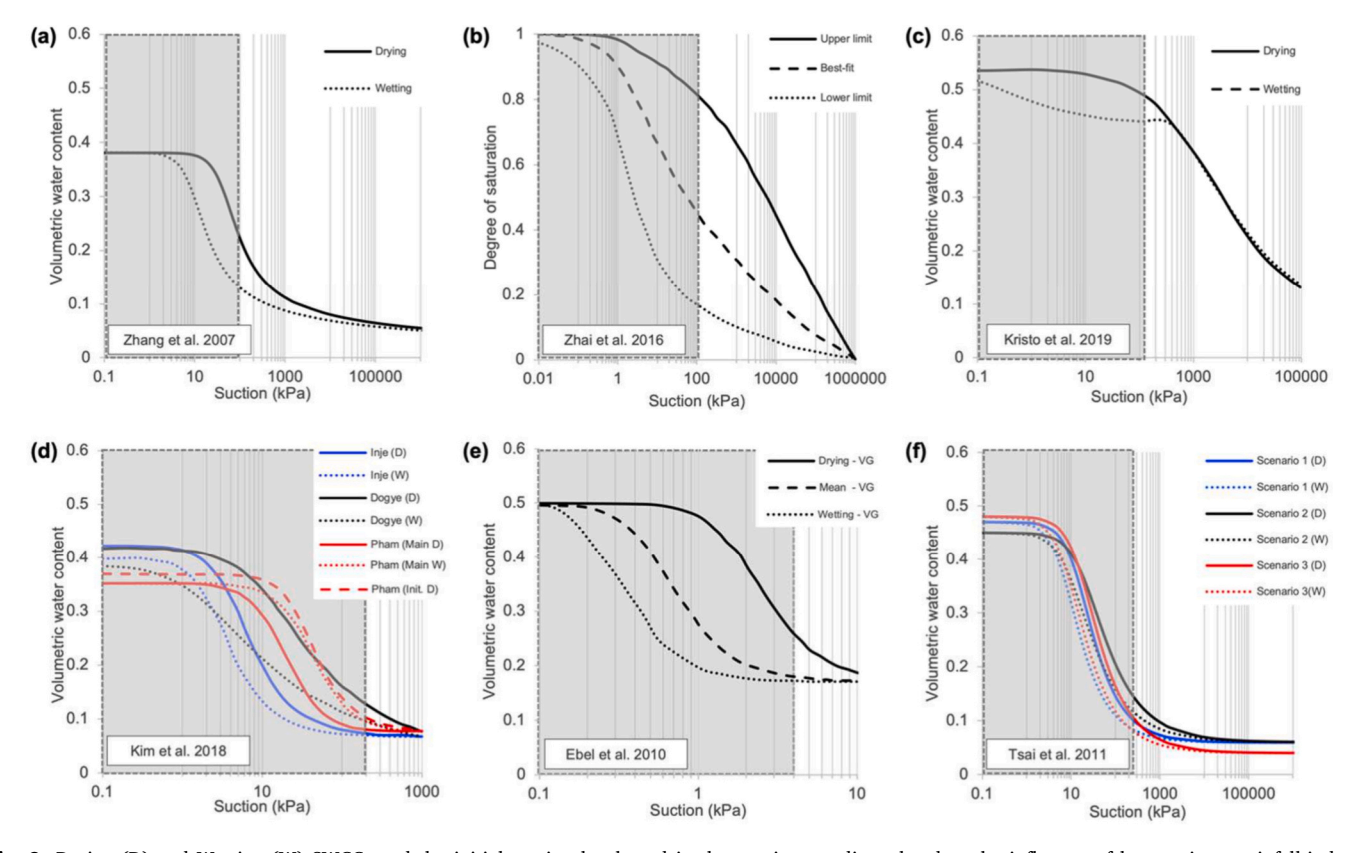


Fig. 3. Drying (D) and Wetting (W) SWCCs and the initial suction level used in the previous studies related to the influence of hysteresis on rainfall-induced slope failures.

drying curve, which is often used in practice, gives reasonable results (Kristo et al., 2019; Zhai et al., 2016; Zhang, 2007), whereas others found it to be less conservative (Ebel et al., 2010; Kim et al., 2018; Tsai, 2011). The initial suction levels (grey-shaded area) applied in these studies are shown in Fig. 3 with reference to its SWCC. Interestingly, the studies with the conclusion that the drying curve gives reasonably conservative results for rainfall-induced slope stability analysis have maximum initial suction closer to the air-entry value or up to the middle part of the SWCC curve. On the contrary, studies with maximum initial suction closer to the residual part of SWCC concluded that the wetting curve results in a more conservative analysis. The influence of the assumption used in determining the magnitude of the initial suction and its potential in explaining the diverging views are investigated in this study.

3. Methodology

The influence of rainfall infiltration on slope stability is studied using the finite element method. The transient water pressure resulting from the applied rainfall is solved using the two-dimensional transient water flow theory as follows:

$$m_{w}^{2}\gamma_{w}\frac{\partial h_{t}}{\partial t}=\frac{\partial}{\partial x}\left(-k_{wx}\frac{\partial h_{t}}{\partial x}\right)+\frac{\partial}{\partial y}\left(-k_{wy}\frac{\partial h_{t}}{\partial y}\right)+q\tag{1}$$

where m_w^2 , γ_w , h_t , t, k_{wx} , k_{wy} , and q are the slope of the soil water-characteristic curve, unit weight of water, total head, elapsed time, coefficients of permeability corresponding to the volumetric water content in x-direction and y-direction, and the applied (rainfall) flux, respectively.

The soil water characteristic curve describes the relationship between the water content and suction in the soil, either for the adsorption or desorption process. In this study, the mathematical equation proposed by Fredlund and Xing (1994) with correction factor $C(\psi)=1$, as defined below, describes the SWCC.

$$\theta_{w} = \frac{\theta_{s}}{\left\{\ln\left[e + \left(\frac{w}{a}\right)^{n}\right]\right\}^{m}} \tag{2}$$

where θ_w , θ_s , e, and ψ are the volumetric water content, saturated volumetric water content, natural base of logarithm, and the soil suction. The a, n, and m are fitting parameters related to the suction value at the inflection point and closely related to the air-entry value, slope of the SWCC at the inflection point, and residual water content, respectively. The permeability function is estimated using Fredlund et al. (1994)'s equation.

The slope stability analysis is performed using the Morgenstern-Price method with the non-linear unsaturated shear strength model (Vanapalli et al., 1996). The equation is defined as follows:

$$\tau = c' + (\sigma_n - u_a) tan \phi' + (u_a - u_w) [S_e tan \phi']$$
 (3)

$$S_e = \left(\frac{\theta_w - \theta_r}{\theta_s - \theta_r}\right) \tag{4}$$

where τ , c', σ_n , u_a , u_w , and ϕ' are the shear strength, effective cohesion, total normal stress, pore air pressure, porewater pressure, and friction angle, respectively. The $(\sigma_n - u_a)$ and $(u_a - u_w)$ correspond to net normal stress on the failure plane and matric suction, respectively. The first, second, and third components in eq. (3) account for the contribution of cohesive, frictional, and suction strength to the soil, respectively. The effective degree of saturation S_e is responsible for quantifying the non-linear contribution of the suction to the shear strength, where θ is the volumetric water content and the subscripts w, r, and s indicate the current, residual, and saturated conditions, respectively.

3.1. Model setup

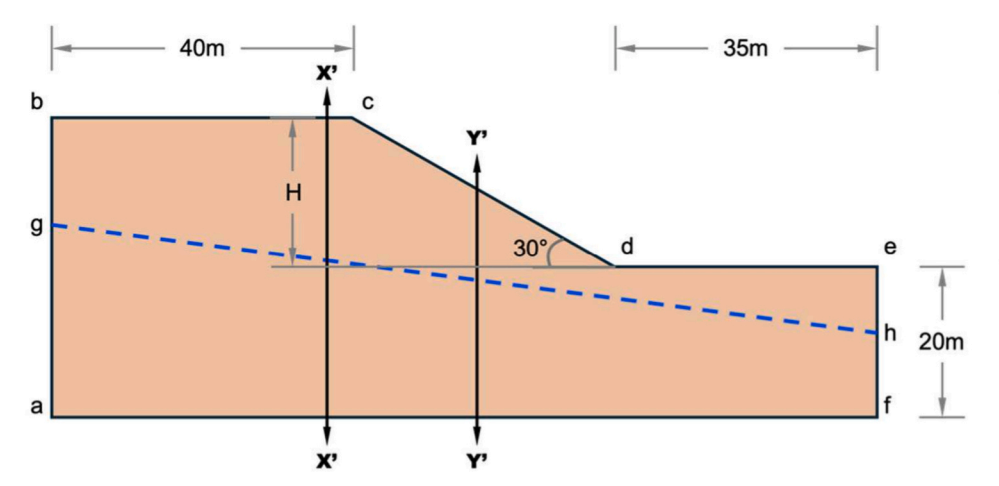
The seepage analysis is conducted using SEEP/W while the slope stability evaluation is conducted using SLOPE/W (GeoSlope, 2018). The slope geometry for analysis is shown in Fig. 4, which is considered typical in Hong Kong (Zhang et al., 2016). The slope is a homogeneous slope with an inclination angle of 30° . The initial groundwater table is applied by drawing a piezometric surface (blue line). A zero-flux boundary is applied on the left and right boundaries above the groundwater table and the bottom of the slope to allow drainage. A constant head is applied along the left and right boundaries below the groundwater table. The rainfall is applied as water flux throughout the slope surface, and excess infiltration water is treated as runoff. In order to explore the influence of SWCC selection and hysteresis on the seepage and stability under the drying and wetting process, the applied rainfall consists of two cycles of rainfall and no-rainfall periods. For each cycle, a six-hour rainfall is followed by a six-hour no-rainfall period. For practical reasons, the effect of evaporation is not modelled during the norainfall period in this study.

3.2. Validation

The validation is done by simulating the field measurement results of a cut slope in Ma On Shan, Hong Kong (Li, 2003). The slope angle is about 30° and the slope height is 17.5 m after the excavation. The slope is mainly comprised of saprolite soil, the typical local Completely Decomposed Granite (CDG) overlying Highly Decomposed Granite (HDG) and then Moderately Decomposed Granite (MDG). The geological cross-section of the slope and the slope geometry used in the verification process are shown in Fig. 5(a) and Fig. 4, respectively. The groundwater table in the model was set such to agree with the field measurement results. The markers in Fig. 5(b)-5(e) show the data points collected from the field monitoring from 16 July 2002 to 19 July 2002 near the crest and the mid-slope, which corresponds to cross-sections X'-X' and Y'-Y' in Fig. 4, respectively. The period is selected as there was a heavy rainfall of 128.5 mm on 17 July 2002.

The initial maximum suction is set to be -10 kPa and a 4-day antecedent rainfall is applied to simulate the porewater pressure profile on 16 July 2002. The saturated permeability of the soil is set to be 5×10^{-6} m/s. Li (2003) adopted the laboratory measured wetting SWCC as it agrees with field measurement results at the slope's crest at 2 m deep (see Fig. 2). Fig. 5(b) and (d) show the numerical results obtained by using the laboratory measured wetting SWCC. The letters F and M in the bracket stand for field measurements and modelling results, respectively. Compared with the field measurement, the simulated porewater pressure follows a similar trend as described in the literature and agrees with the final porewater pressure profile. After the rainfall on 17 July 2002, the porewater pressure at immediate depths (<1 m) increased, although no perched water pressure was developed. As lower rainfall intensity was observed on the following days (18-19 July 2002), the porewater pressure at the immediate depths (<1 m) decreased. The water within the soil was redistributed into deeper layers, causing an increase in the porewater pressure at 2-3 m depths. Additionally, no groundwater table rise was observed due to the heavy rainfall.

Fig. 2 illustrates the hysteresis phenomenon observed in the laboratory measurements and the variability observed in the field measurements. The variability might be attributed to the difference in stress level and particle gradation observed in the crest and berm area, as reported in the literature. Another numerical analysis using drying SWCC is adopted to illustrate the influence of SWCC selection in the analysis. As shown in Fig. 5(c) and (e), the porewater pressure follows a similar trend with the field measurement. While it provides a better agreement on the final profile (19/7) plotted at the crest, the simulation results might overestimate the porewater pressure at the mid-slope.



	Validation	Test cases
Н	17.5 m	20 m
ag	30 m	20 m
hf	12 m	10 m

Boundary conditions:

- · bc, cd, de = Rainfall flux, q
- bg, eh, af = no flow boundary (Q = 0 m³/s)
- ag, hf = total water head at the side

Fig. 4. Slope geometry used in the validation and the study.

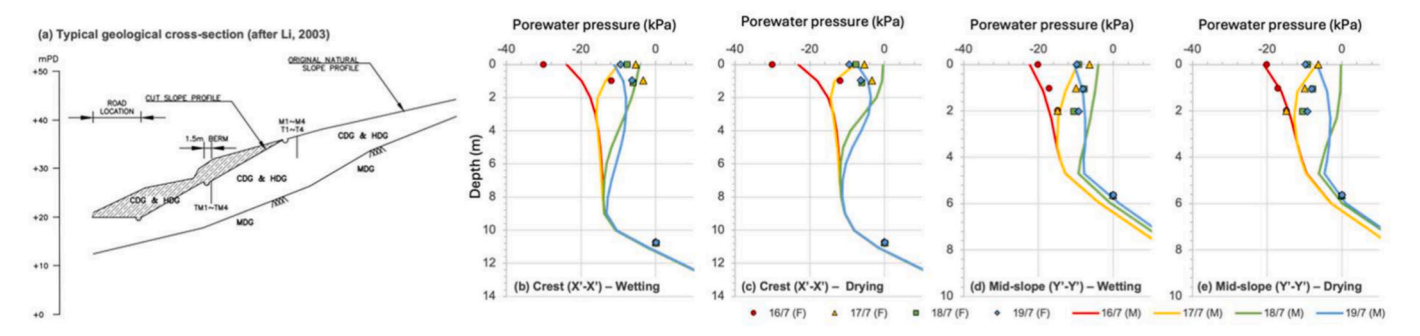


Fig. 5. Numerical validation and comparison of the numerical results using wetting and drying SWCC.

3.3. Parametric study

Fig. 1 and Fig. 2 show the typical shape and relationship of the drying and wetting curves. Mathematical expressions are sometimes adopted to represent the SWCC and facilitate analysis. In this study, the influence of the approach adopted regarding hysteresis, such as the selection of the SWCC towards the rainfall-induced slope stability analysis, is evaluated. Different SWCC shapes, attained by varying the fitting parameters a, n, m, and θ_s of the SWCC (Fredlund and Xing, 1994), are generated to represent the drying and wetting SWCC. The equation was originally proposed to represent the drying SWCC, and it was considered the most appropriate best-fit equation for a wide range of soils over the entire matric suction range (Leong and Rahardjo, 1997). However, for practical reasons, the mathematical expression was also used to represent the wetting curve in the previous studies (Kristo et al., 2019; Tami et al., 2004; Zhang, 2007).

The air-entry value (AEV) is the magnitude of suction required to desaturate the largest pore in the soil, beyond which air will start entering the pores of the saturated soil. The AEV of the drying curve is typically located at a higher suction than in the wetting curve. The parameter a is closely related to the AEV of the soil and increases as the AEV increases, which shifts the SWCC to a higher magnitude of matric suction without changing the overall shape (steepness) of SWCC. The parameters n and m are related to the gradient of the SWCC at the inflection point and residual water content, respectively. The steepness of the SWCC controls the rate at which the soil desaturates or saturates for every change in the matric suction due to the drying or wetting process, respectively. As shown in Fig. 1 and Fig. 2, the drying curve typically has a steeper SWCC than the wetting curve. Subsequently, the drying curve typically has a higher n. Additionally, parameter m is lower when the residual water content increases, and thus, the drying curve generally

has a lower parameter *m*. These observations are confirmed through previous studies (Fredlund, 2015; Pham et al., 2005; Yang et al., 2004; Zhang, 2007) and are used to design the parametric study.

Table 1 summarizes the parametric study test cases used in this study to investigate the influence of different SWCC shapes on rainfall-induced slope instability. By varying the fitting parameters listed in Table 1, SWCC shapes resembling drying relative to wetting, or vice versa, can be obtained, and its influence when adopted in rainfall-induced slope stability analysis can be examined. Note that the drying curve typically exhibits a lower parameter m compared to the wetting curve, while parameters a, n, and θ_s are generally higher in the drying curve. Additionally, the role of rainfall intensity in terms of the water flux to saturated permeability ratio, q/k_{sat} , is also investigated for a wide range. The variation of SWCC and permeability for different input parameters is shown in Fig. 6, which covers a reasonably wide range as compared with literature studies. More than 300 test cases are examined in this study. The input parameters used in the numerical analysis are summarized in Table 2. As will be shown later, the wide range of SWCC parameters, rainfall intensity, permeability and initial suction adopted and the very large number of scenarios analyzed lead to more meaningful and comprehensive results, and these results offer insights into the intricate interplays of the various factors.

In the unsaturated slope stability analysis, the magnitude of maximum initial suction is usually treated as either a user's input or assumed to be hydrostatic. Fig. 3 shows the variation of presumed maximum initial suction, which ranges from 5 kPa to 250 kPa (from hydrostatic assumption). As discussed in the earlier section, it is important to explore the possible influence of the magnitude of initial suction in relation to the SWCC shape on the rainfall-induced stability analysis. The magnitude of the initial suction is critical in influencing the strength and permeability of the soil, especially those located at the

Table 1 Summary of parametric study.

	Test cases	а	n	т	θ_s	Initial suction (kPa)	Rainfall
1	Influence of parameter a	$\begin{bmatrix} 1 \\ 10 \\ 100 \end{bmatrix}$	2	1	0.4	50	$\left[egin{array}{l} q=0.5\ k_{sat}\ q=1\ k_{sat}\ q=3\ k_{sat} \end{array} ight]$
2	Influence of parameter n	1000 ¹ 100	$\begin{bmatrix} 2\\3\\4 \end{bmatrix}$	1	0.4	50	$\left[egin{array}{l} q=0.5k_{sat}\ q=1k_{sat}\ q=3k_{sat} \end{array} ight]$
3	Influence of parameter m	100	2	$\begin{bmatrix} 1 \\ 2 \\ 5 \end{bmatrix}$	0.4	50	$\left[egin{array}{l} q=0.5k_{sat}\ q=1k_{sat}\ q=3k_{sat} \end{array} ight]$
4	Influence of saturated volumetric water content θ_s	100	2	1	$\begin{bmatrix} 0.3\\0.4\\0.5 \end{bmatrix}$	50	$\left[egin{array}{l} q=0.5k_{sat}\ q=1k_{sat}\ q=3k_{sat} \end{array} ight]$
5	Influence of initial suction	$\begin{bmatrix} 10 \\ 50 \\ 100 \end{bmatrix}$	2	1	0.4	$\begin{bmatrix} 10 \\ 50 \\ 100 \end{bmatrix}$	$\begin{bmatrix} q = 0.5 k_{sat} \\ q = 1 k_{sat} \\ q = 3 k_{sat} \end{bmatrix}$

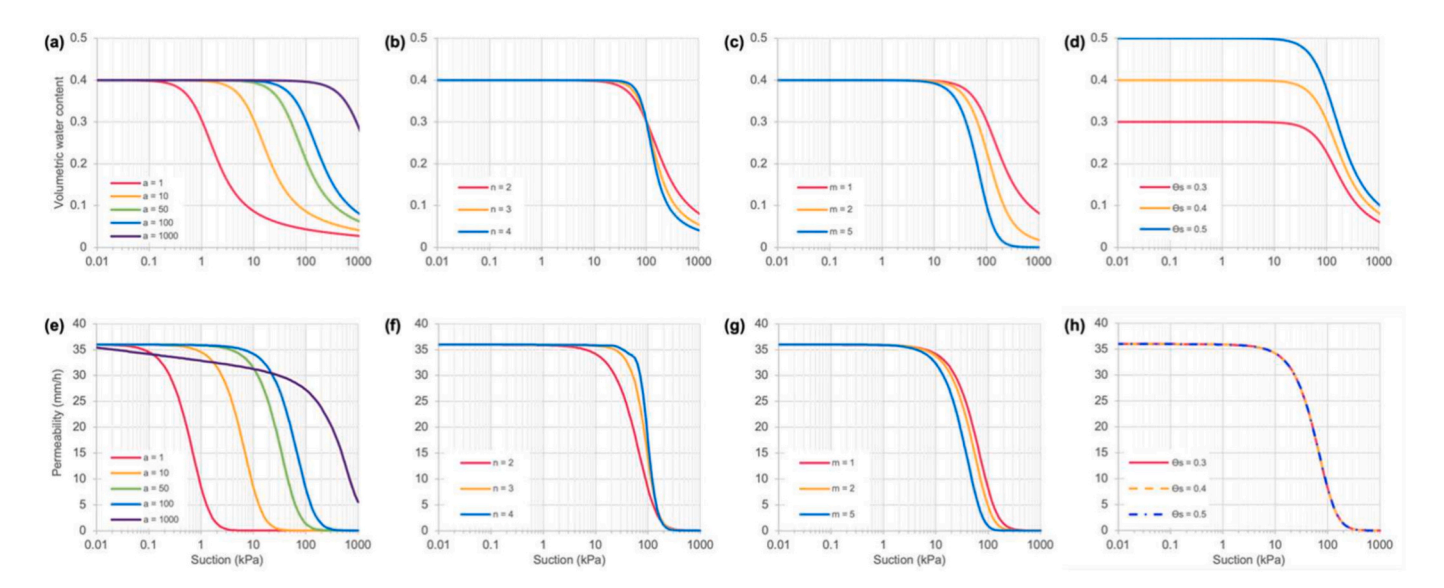


Fig. 6. SWCC and permeability functions used in the parametric study.

Table 2
Input parameters used in this study.

Parameter	Parametric study
Cohesion, c' (kPa)	2
Friction angle, ϕ' (°)	35
Unit weight (kN/m³)	18
Saturated permeability, k_s (mm/h)	36
Maximum suction (kPa)	50 (unless specified)

shallow depths, which are critical against rainfall-induced failures. In this study, the initial condition will be assumed as hydrostatic with a maximum suction of 50 kPa except when it is specified (test cases series 5)

4. Numerical study illustrating influence of the selection of SWCC

4.1. Influence of different soil water characteristic curve on slope stability

4.1.1. Effect of air-entry value on the slope stability

As illustrated in Fig. 6(a), the higher parameter a implies a higher AEV, which resembles the drying SWCC relative to the wetting SWCC. As

the initial suction is set to be 50 kPa, the soil with higher *a* will have a higher initial water content (Fig. 6(a)) and, subsequently, a higher shear strength (Eq. (3)) and initial FOS (see Fig. 7).

When rainfall commences, water infiltrates the slope. If the amount of water flowing into the soil is larger than that flowing out, the matric suction decreases, which consequently, reduces the soil strength. The infiltrated water also potentially causes seepage force that might destabilize the slope. Likewise, when the rainfall stops, the suction might regain, and the slope stability will increase.

Fig. 7 (a), (e), and (i) summarize the variation of safety factor obtained from the critical slip surface with time when the parameters a and q/k_s ratio vary. Throughout the rainfall (grey-shaded areas) and norainfall (white areas) periods, the slopes with higher a experience more significant decreases and increases in terms of safety factor, respectively. On the contrary, the stability of the slope with lower a tends to be constant. As the shape of SWCC influences the permeability function, when the initial suction is 50 kPa, soils with higher a will generally have higher permeability. When the permeability is high, more water can easily infiltrate the soil. This explains the higher fluctuation in terms of safety factors for soils with higher a, which agrees with the behavior of the slope stability when the drying curve is adopted, as observed in a previous study (Zhang, 2007). However, higher a does not necessarily guarantee a more conservative analysis, as shown

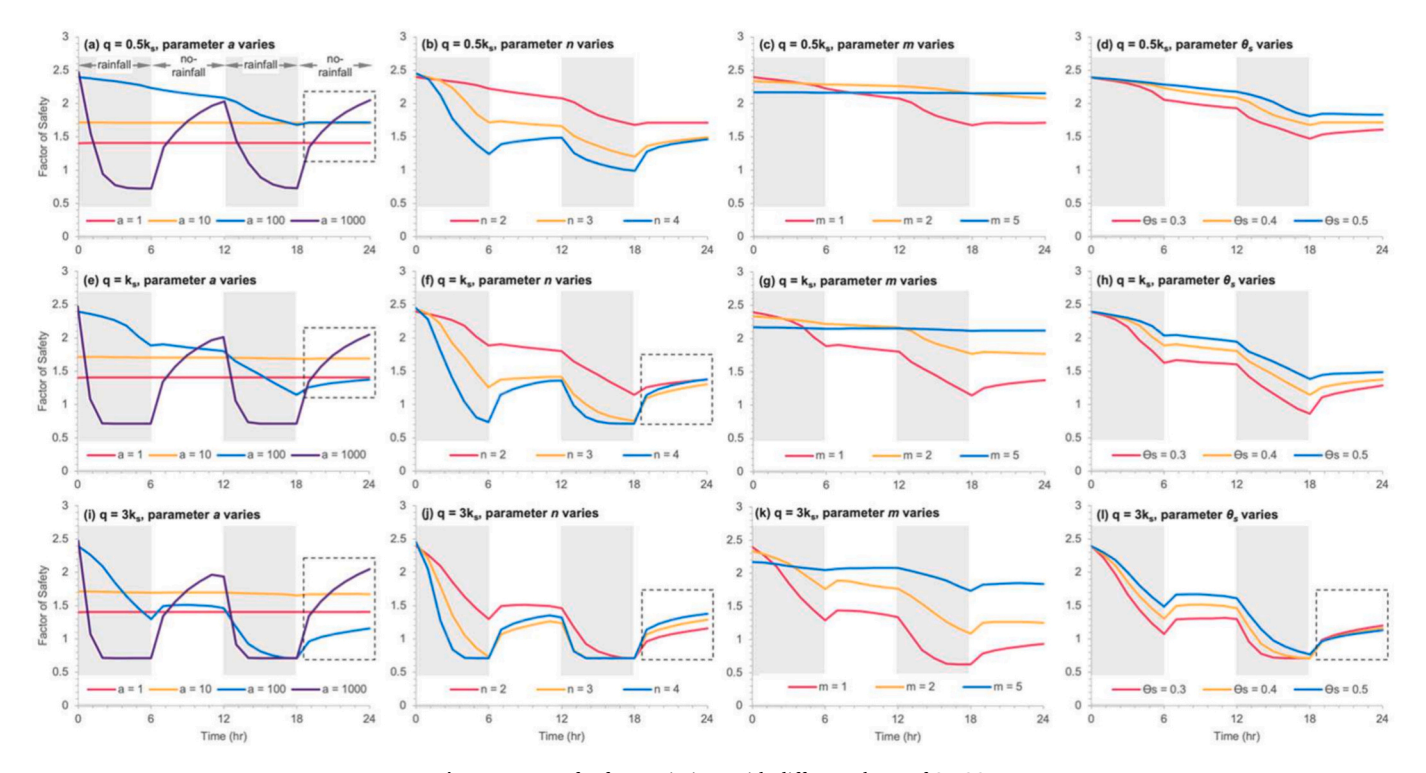


Fig. 7. Factor of safety variations with different shape of SWCC.

by the dotted boxes in Fig. 7 (a), (e), and (i). In such a case, the reliability of SWCC in representing the actual soil needs to be ensured, or else the calculation results might overestimate the safety factor under the rainfall while subsequently underestimate the influence in the no-rainfall period.

4.1.2. Effect of the slope of SWCC on the slope stability

The influence of the slope of SWCC near the inflection points is studied by varying the parameter n. The saturation and desaturation rate increases as the parameter n increases. Fig. 6 (b) and (f) show that the relationship between the suction and the volumetric water content or the permeability, when n varies, does not bear a monotonic decrease or increase. For the SWCCs used in this study, a higher n results in a higher volumetric water content when the suction is smaller than 100 kPa. Likewise, when suction is larger than 100 kPa, under the same magnitude of suction, the soil with higher n will have lower volumetric water content.

In this study, the maximum initial suction within the slope is assumed to be 50 kPa. Consequently, soil with higher n will have higher initial volumetric water content and permeability. Fig. 7 (b), (f), and (j) summarize the influence of different n on the slope stability when subjected to various rainfall scenarios. Slopes with higher n have higher initial FOS and a more significant fluctuation of slope stability under cycles of rainfall and no-rainfall periods. The behavior is even more significant when the slope is subjected to high-intensity rainfall. Additionally, the slopes with higher n require shorter time to reach the minimum FOS. It is interesting, however, that when the slope with n=2 is subjected to lower rainfall intensity, the safety factor continuously decreases, even when the rainfall stops. The observations show that the shape of SWCC not only influences the magnitude of the minimum safety factor but also the time of failure and the rate of safety factor decrease and increase.

The slope of SWCC closer to the residual zone is controlled by parameter m. Fig. 6 (c) and (g) show that a higher m results in a steeper SWCC, and for the same magnitude of suction, soil with higher m will have a lower volumetric water content and permeability. Fig. 7 (c), (g), and (k) show the variation of safety factor with time for soil with

different magnitudes of m. In the first rainfall cycle of lower intensity rainfall (Fig. 7(c)), the slope with higher m is more critical, attributed to the lower initial FOS. As the rainfall intensity continues, the slope with lower m results in a lower safety factor but is also more sensitive towards rainfall patterns. The results shown in Fig. 7 indicate that slopes with steeper gradient of SWCC and higher residual water content, which correspond to the drying curves relative to the wetting curve, result in lower FOS with more significant FOS rebound.

4.1.3. Effect of saturated volumetric water content on the slope stability

When the SWCC parameters and the saturated permeability k_s are assumed to be identical except for the magnitude of saturated volumetric water content, θ_s , the permeability function estimated from the SWCC of the soils is identical (Fig. 6 (d) and (h)). It should be noted, however, that despite having an identical permeability function, the transient permeability of soil having different θ_s will not be the same throughout the analysis. A previous study noted that soils with larger effective water content, $(\theta_s - \theta_r)$, can store more water and require more water to reach a fully saturated state. Subsequently, the matric suction will take longer to dissipate (Zhang et al., 2016). Fig. 7 (d), (h), and (l) summarize the variation of safety factors for soils with different magnitudes of θ_s . The analysis shows that slopes adopting SWCC with lower θ_s , such as the wetting SWCC relative to the drying SWCC, will experience lower slope stability and fluctuate more when subjected to rainfall and no-rainfall periods.

4.2. Influence of assumption related to the initial suction

As summarized in the previous section, the conclusions obtained from previous studies on selecting SWCC, especially considering the hysteretic behavior, are diverging. Interestingly, studies that consider the drying curve to be more conservative tend to have initial suction closer to the air-entry value (Kristo et al., 2019; Zhai et al., 2016; Zhang, 2007). In contrast, when the magnitude of the initial suction is closer to the residual zone, the wetting curve is concluded to be more conservative (see Fig. 3). This section will discuss the role of the initial suction on the rainfall-induced slope failure analysis. In the present study, only the

variation of parameter *a* represents the hysteretic behavior to reduce the variable. Generally, the drying curve will have higher AEV and, subsequently, higher parameter *a* compared to the wetting curve.

Fig. 8 summarizes the safety factor of the slope with varying initial suction and parameter a when subjected to two cycles of rainfall (greyshaded areas) and no-rainfall periods. Three values of a are selected, 10, 50, and 100, to represent the variation of SWCC. Likewise, three magnitudes of initial suction, 10 kPa, 50 kPa, and hydrostatic condition are assumed. Based on the slope geometry, the hydrostatic condition results in a maximum suction of around 235 kPa.

The results in Fig. 8 show that the initial suction and parameter a influence the initial safety factor. For the same a, the slope with higher initial suction will have higher initial safety factor. Higher suction contributes to a higher suction strength component and a higher effective degree of saturation S_e , both of which contribute to the overall shear strength (see Eq. (3)). Additionally, for the same initial suction, the slope with higher a will have higher initial FOS. The difference between the initial FOS of slopes with different a increases as the initial suction increases

Similar to the previous observation, the reduction in terms of safety factor increases with the rainfall intensity. As a result, under low-intensity rainfall, slopes with lower initial safety factors will inherently give more conservative results. For all three rainfall cases across different magnitudes of initial suction, the lowest minimum safety factor is reached by the slope having a=100 across all initial suctions. The exception is for the hydrostatic cases, where the slope with a=10 gives the lowest safety factor when subjected to rainfall intensities of $0.5k_s$ and k_s . Consistent with observation in previous sections, slopes with higher values of a, which resemble the drying SWCC relative to the wetting SWCC, generally experience a more prominent fluctuation in terms of safety factor, especially when subjected to high-intensity rainfall.

To further understand the role of the selected SWCC and suction level to the slope stability, the porewater pressure profile at cross-section Y'-Y' located at the mid-slope (see Fig. 4), when subjected to rainfall of $q=k_s$ (36 mm/h), is plotted in Fig. 9 with a time interval of 3 h. As the rainfall occurs from 0 h - 6 h, the rainwater infiltrates the slope, causing a reduction in terms of matric suction. The matric suction regains when the rainfall stops as the no-rainfall period proceeds from 6 h - 12 h, and the infiltrated water is redistributed to deeper depths. This behavior repeated under the second cycle of rainfall and no-rainfall period on 12 h -18 h and 18 h - 24 h, respectively. The slope having higher a generally has a deeper wetting front and loses its suction faster, which is consistent with previous studies (Tsai, 2011; Zhai et al., 2016).

The results also show agreement with previous observations on the seepage behavior affected by different magnitudes of initial suction (Tsaparas et al., 2002). They observed that slopes with high initial suction experience a considerable reduction of matric suction at shallow depths compared to those for lower initial suction. However, soils with higher initial suction can maintain their suction better at deeper depths.

Additionally, Freeze (1969) concluded that out of all parameters controlling the infiltration and groundwater recharge, it is likely that the antecedent soil moisture regime, which is related to the magnitude of initial suction, is the most important. They noted that soil with the wettest profile (i.e., having a lower suction) will need a much shorter time to reach saturation and a deeper wetting front. This explains why slopes with lower initial suction exhibit a more significant reduction of FOS.

Fig. 10 shows the seepage profiles and the slip surfaces of the slope under rainfall intensity of 36 mm/h ($q = k_s$) at a calculation time of 18 h. Since the location of the initial groundwater table is identical for all the cases, the only difference in the initial condition is the SWCC and the magnitude of the initial suction. The figure shows that the slope with higher a generally has a deeper initial slip surface. As the rainfall happens, the slope with higher a loses its suction more significantly, which in some cases also causes an increase in the groundwater table. The slip surface at the calculation time of 18 h is also plotted as red lines in Fig. 10. Slopes with higher initial suction generally have a deeper slip surface. Additionally, the critical slip surface of slopes with higher a tend to move closer to the toe. As shown in Fig. 9, slopes with higher parameter a tend to have a deeper wetting front and even potentially cause the groundwater level to rise, thus offering a potential explanation for the observed phenomenon. This highlights the intricacy of the factors causing rainfall-induced slope failures.

5. Discussion

5.1. The assumption of initial suction in explaining the diverging views

The magnitude of the matric suction in the field can be influenced by various factors such as soil type and climatic conditions. Field measurements of saprolitic hillside, colluvium slope, weathered rhyolite, and weathered granite in Hong Kong (Li, 2003; Ng et al., 2011; Zhang et al., 2016) indicate that the suction ranges from zero to 80 kPa near the surface area, depending on the weather conditions. After a long dry period, field measurements in tropical regions, such as Singapore, observed the matric suction of around 50 kPa (Tsaparas et al., 2002). Meanwhile, the matric suction in a slope in Switzerland can be as high as 100 kPa (Springman et al., 2013). In practical applications, it is common to assume that the porewater pressure profile is hydrostatic. However, this assumption might not be appropriate when the groundwater table is deep.

The hysteretic characteristic results in different SWCC, depending on the process experienced by the soil, i.e., whether it is wetting or drying. Moreover, numerous drying and wetting scanning curves can also exist within the main drying and wetting SWCCs. By varying parameter a, the parametric study here attempts to understand the influence of selecting a particular shape of SWCC out of the family of SWCCs generated due to the hysteretic characteristics. As the drying curve typically has higher AEV, slopes with higher parameter a can be used as a reference of the

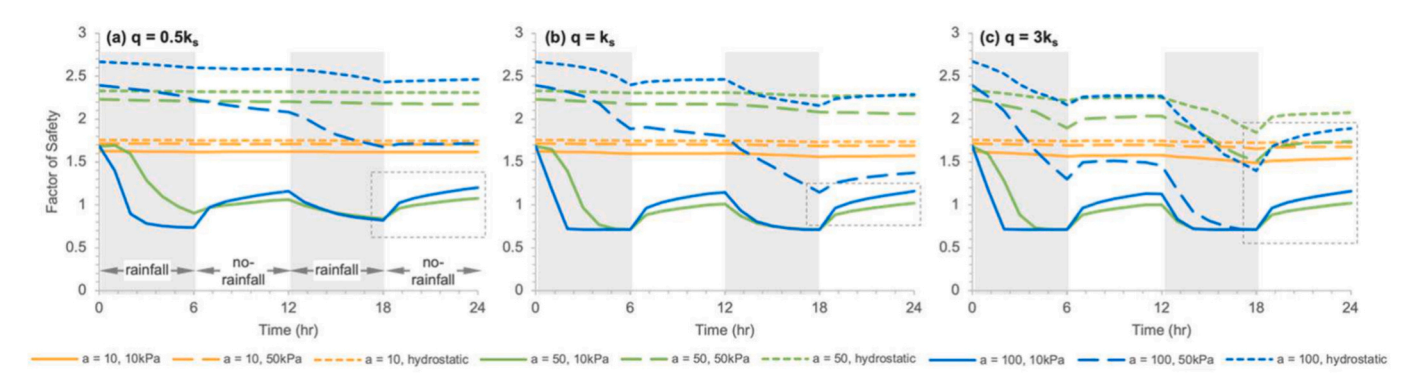


Fig. 8. Safety factor of the slope with various initial suction and varying parameter a when subjected to different rainfall intensities.

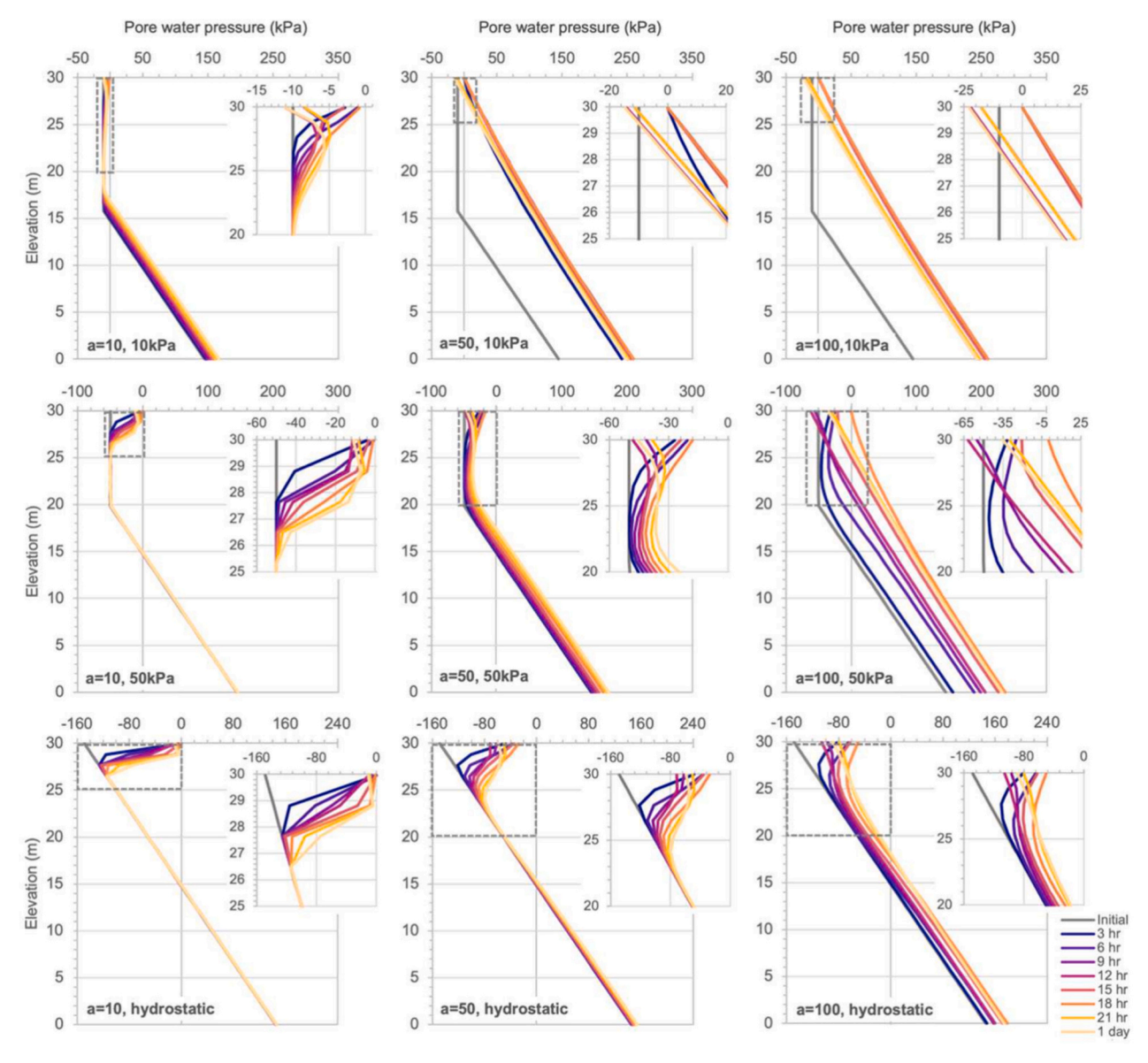


Fig. 9. Porewater pressure profile under rainfall intensity of 36 mm/h ($q = k_s$).

drying SWCC compared to the wetting SWCC. The results in Fig. 11 potentially explain the diverging views related to the SWCC selection discussed in Section 2.

The influence of the magnitude of maximum initial suction is investigated by studying the stability of the slope before and after experiencing two cycles of 6-h rainfall events (0–6 h and 12–18 h) followed by 6 h of no-rainfall event. The results are plotted in Fig. 11. The empty square, circle, and triangle markers represent the initial safety factor of slopes with parameter a of 10, 50, and 100 kPa, respectively. As the maximum initial suction increases, the initial safety factor increases. This is consistent with previous laboratory measurements: soils with higher air-entry values will have higher shear strength, and the shear strength increases with the magnitude of suction (Vanapalli et al., 1996). Additionally, the figure also shows that the influence of maximum initial suction on the initial FOS is more prominent in slopes with higher a. Nonetheless, all of the cases have high initial FOS, ranging from 1.5 to 2.75.

The solid markers in Fig. 11 represent the minimum FOS experienced by the slope when subjected to the rainfall event. The figure shows that when lower initial suction is assumed, the slope with higher a to resemble the drying curve relative to the wetting curve, tends to give a

more conservative analysis. As the maximum initial suction increases, the slope with lower a has the lowest FOS, which is mostly attributed to its low initial FOS (see Fig. 8(a) and (b); Fig. 11(a) and (b)). For instance, when the slope is subjected to low-intensity rainfall (Fig. 11(a)), the slope with parameter a=100 (blue triangle) gives the lowest FOS when the initial suction ranges from 10 to 50 kPa. However, as the maximum initial suction increases above 50 kPa, the slope with parameter a=10 (pink square) is more conservative, mainly attributed to the low initial FOS and less FOS reduction it experienced during rainfall (dotted yellow line in Fig. 8(a)). Similarly, slopes with a=100 (blue triangle) provide conservative estimates for suction below 80 kPa and all ranges of suction when subjected to intermediate- (Fig. 11(b)) and high-intensity (Fig. 11 (c)) rainfall, respectively.

The results presented in Fig. 11 illustrate the complex interplay of the relevant factors including the magnitude of initial suction, SWCC (parameter *a*), rainfall intensity, and rainfall pattern in the evaluation of rainfall-induced slope failures.

The results confirm the observations discussed in Section 2: Studies that concluded the drying curve to be more conservative tend to have initial suction closer to the air-entry value or up to the mid-section of the SWCC. Conversely, studies with higher initial suction closer to the

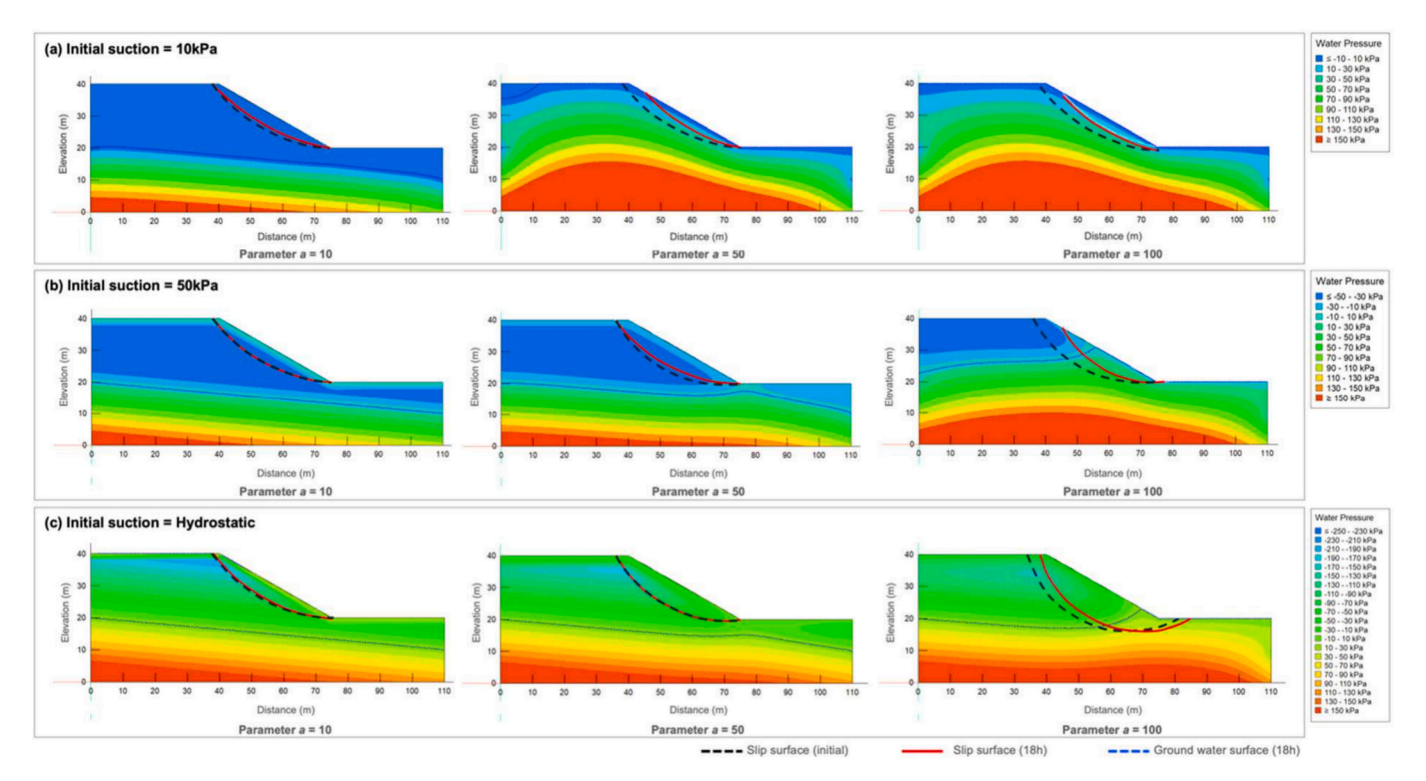


Fig. 10. Seepage and slip surface profiles under rainfall intensity of 36 mm/h ($q = k_s$) at calculation time of 18 h.

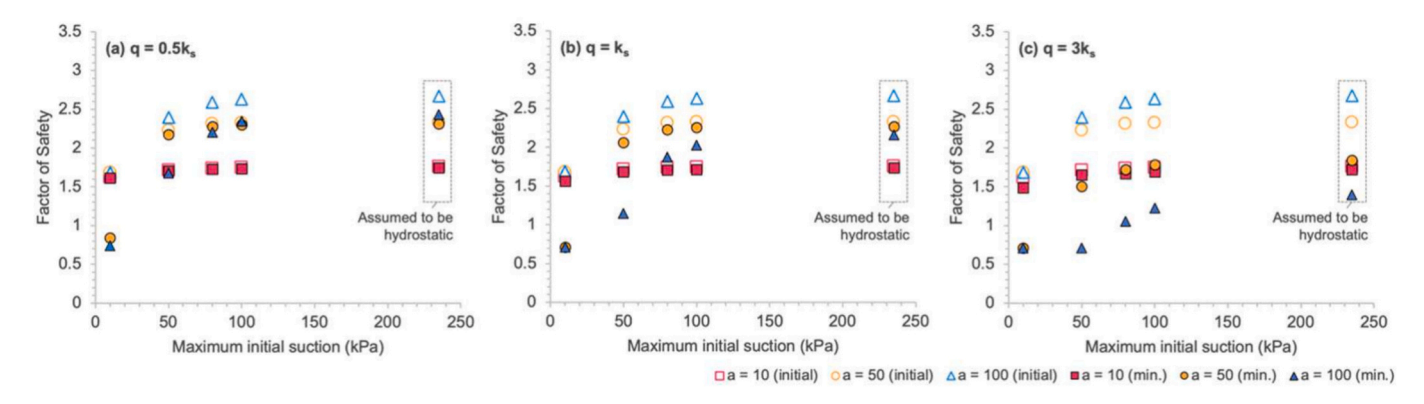


Fig. 11. Influence of maximum initial suction on factor of safety against different rainfall intensity.

residual part of the SWCC tend to conclude that the wetting curve is more conservative. When the initial suction is lower or equal to 80 kPa, which is closer to the air-entry value of all the SWCCs (see Fig. 6(a)), the test cases having a=100 give the most conservative analysis (Fig. 11(a) and (b)). As the suction increases and becomes closer to the residual values, test cases with lower air-entry values, resembling wetting curves, give lower FOS results. However, Fig. 11(c) shows that slopes with higher air-entry values, resembling drying SWCC, result in the lowest FOS as the rainfall intensity increases, regardless of the magnitude of the initial suction. Thus, the influence of the magnitude of the initial suction relative to the air-entry value towards the SWCC selection reduces as the rainfall intensity increases.

It should be noted, however, that rainfall-induced slope instability can be influenced by many other factors and their interaction with each other, as shown in many previous studies (Ering and Babu, 2016; Natalia and Yang, 2022), among others. Nevertheless, the magnitude of the initial suction can influence the slope's initial volumetric water content and permeability, which subsequently controls the amount of water infiltrating or evaporating into or from the slope. This provides a

possible explanation for the diverging conclusions in previous studies related to the influence of hysteresis on slope stability. The numerical results indicate that it is not the magnitude of the initial suction alone but its relationship with the SWCC which controls the influence of hysteresis on rainfall-induced slope failure.

5.2. Influence of soil permeability and rainfall intensity

Fig. 12 summarizes the influence of the SWCC parameter selection and the maximum initial suction for different permeability and rainfall intensities test cases in terms of q/k_s . It is assumed that the slopes are subjected to 6 h of rainfall and no-rainfall periods, followed by another 6 h of rainfall. The vertical lines represent the standard deviation of the normalized FOS at the end of calculation at t=18 h (FOS_{t=18h} / FOS_{t=0h}), taken from five different test cases of maximum initial suction: 10 kPa, 50 kPa, 80 kPa, 100 kPa, and hydrostatic assumption. The straight lines represent the trend of the normalized FOS in all five test cases against various q/k_s .

The results in Fig. 12 show that the normalized FOS decreases when

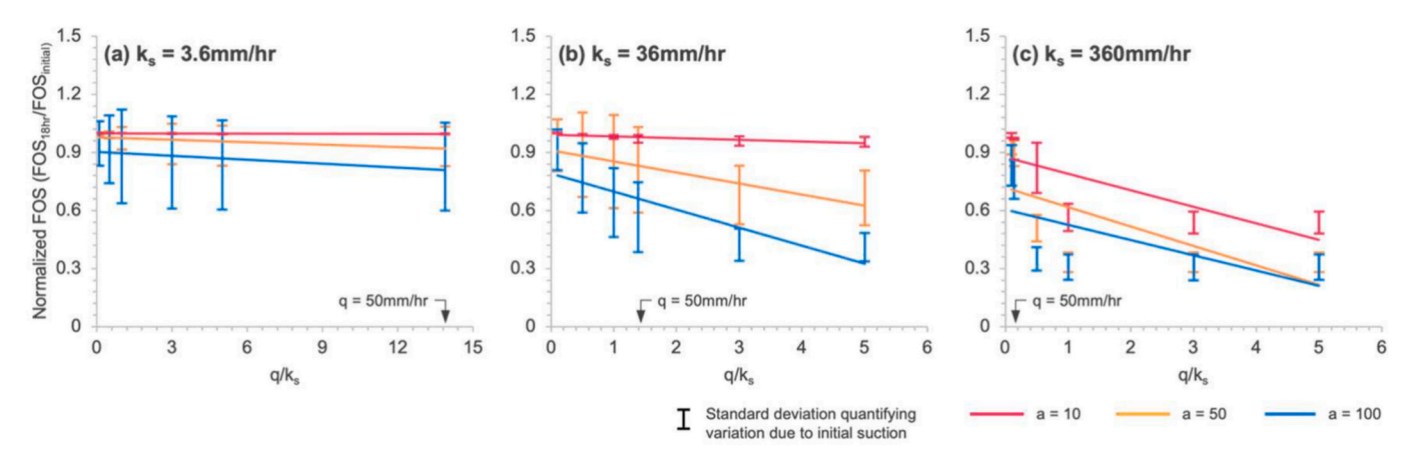


Fig. 12. Influence of saturated permeability on the normalized factor of safety at calculation time of 18 h.

the saturated permeability increases. Additionally, the slope stability against transient rainfall seems to be related to the absolute intensity of the rainfall and the soil properties instead of the q/k_s ratio. For slopes with lower a, resembling the wetting SWCC, the influence of different magnitudes of initial suction is less significant when the saturated permeability is 3.6 mm/h and 36 mm/h. However, more significant variations can be observed in soils with high permeability. On the contrary, when a = 100, the variation in terms of normalized FOS becomes less significant when the saturated permeability is high. One of the possible reasons is that soils with lower a have initial FOS that are closer to each other regardless of the initial suction, and the FOS fluctuates less significantly throughout the rainfall events (see Fig. 8). However, when the permeability is high, the reduction of FOS is more significant, thus causing more variation in terms of $FOS_{t=18h}$ for different magnitude of initial suction. In contrast, the initial FOS of soil with higher a, which reflects the drying curve features, can vary significantly depending on the magnitude of initial suction. For low to intermediate permeability, the FOS_{t=18h} varies depending on the initial suction and the rainfall intensity. Nevertheless, when the soil has high permeability, most cases experience significant reduction in FOS, which tends to be lower than 1.0; thus, less variation in terms of $FOS_{t=18h}$ are observed.

5.3. On the definition of conservative design

In the parametric study, the slopes are subjected to two cycles of rainfall and no-rainfall periods. During the rainfall period, the rainwater infiltrates the slope and potentially reduces the safety factor. Likewise, when the rainfall stops for a particular duration, the soil regains its suction and potentially increasing the safety factor. In the design process, conservative designs are commonly done by selecting scenarios with the lowest minimum safety factor. However, the numerical results show that in some test cases, the scenarios that produce the most critical safety factor under rainfall might regain their strength and have a safety factor higher than that of less critical cases during the no-rainfall period. Examples of these observations are denoted by grey dotted boxes in Fig. 7 and Fig. 8. Similar results were exhibited in previous studies (Ebel et al., 2010; Kristo et al., 2019).

When designing against rainfall-induced slope failure, most design practices focus only on designing against rainfall by applying certain rainfall intensities, and the no-rainfall period is usually ignored. In such cases, designing using soil parameters resembling the drying SWCC, such as lower magnitude of m values and higher values of a, n, and θ_s , generally gives more conservative results. However, when we consider the hysteretic nature of SWCC and realistic rainfall patterns, including the rainfall and no-rainfall periods, the selection of the conservative scenario needs to be cautiously approached. The study of Natalia and

Yang (2024) highlighted the potential contribution of rainfall patterns and the importance of considering a realistic scenario in slope stability analysis against rainfall-induced failures. Generally, there are two ways to define the critical case: the scenario resulting in the lowest minimum safety factor or the scenario that gives an overall minimum safety factor during rainfall and no-rainfall periods.

The results from this study are useful for understanding the influence of different SWCC shapes when adopted to rainfall-induced slope instability analyses, particularly when considering the influence of hysteresis. The drying and wetting curves are compared by having various magnitudes of parameter a and keeping the slope of SWCC constant. Although it might oversimplify the drying and wetting curves relationship, this approach is consistent with methods proposed in previous studies in estimating the wetting curve from a drying curve. The ratio of the parameter a of the wetting and the drying curves ranges from 0.0034 to 0.2 in these studies (Pham et al., 2005; Zhang, 2007).

Fig. 13 shows the collected SWCC data of typical soils in Hong Kong for Completely Decomposed Granite (CDG) and Completely Decomposed Tuff (CDT) from various laboratory and field measurements published in previous studies (Gan and Fredlund, 1995; Leung, 2011; Li, 2003). As illustrated in Fig. 2 and Fig. 13, the SWCC measurements may vary due to various factors such as heterogeneity, the stress state, particle gradation, and density, adding to the complication alongside its hysteretic nature. The preliminary SWCC envelopes for upper limit (UL), average (average), and lower limit (LL) envelopes are drawn and can be useful for future reference in rainfall-induced slope stability analysis. Moreover, a database of fitting parameters of wetting and drying SWCC for various soil types was available in Pham (2001). Generally, the envelopes are consistent with the previous discussion. The drying curve generally has a higher magnitude of parameters a and b and a lower magnitude of parameter b.

This study shows that rainfall-induced slope instability is inherently complex, involving intricate interplays among various factors. The SWCC can be influenced by factors such as soil type and structure, initial water content, density, mineralogy, and stress level. The findings from this study related to the influence of the relationship between AEV and the magnitude of initial suction can be useful in facilitating the conservative design approach. The results shown in Fig. 11-13 provide preliminary guidance for selecting the SWCC for analysis in subtropical regions like Hong Kong. The typical suction ranges from 0 to 80 kPa (Li, 2003; Ng et al., 2011; Zhang et al., 2016), with permeability varying between 36 mm/h for in-situ soil to 0.036 mm/h for compacted soil (Gan and Fredlund, 1995). The slopes are potentially subjected to highintensity rainfall events of 50 mm/h or higher. Based on the results in Fig. 11-12, one may suggest that the use of higher parameter a, resembling the drying curve relative to the wetting curve, generally offers conservative estimates across a typical range of initial suction (0-80

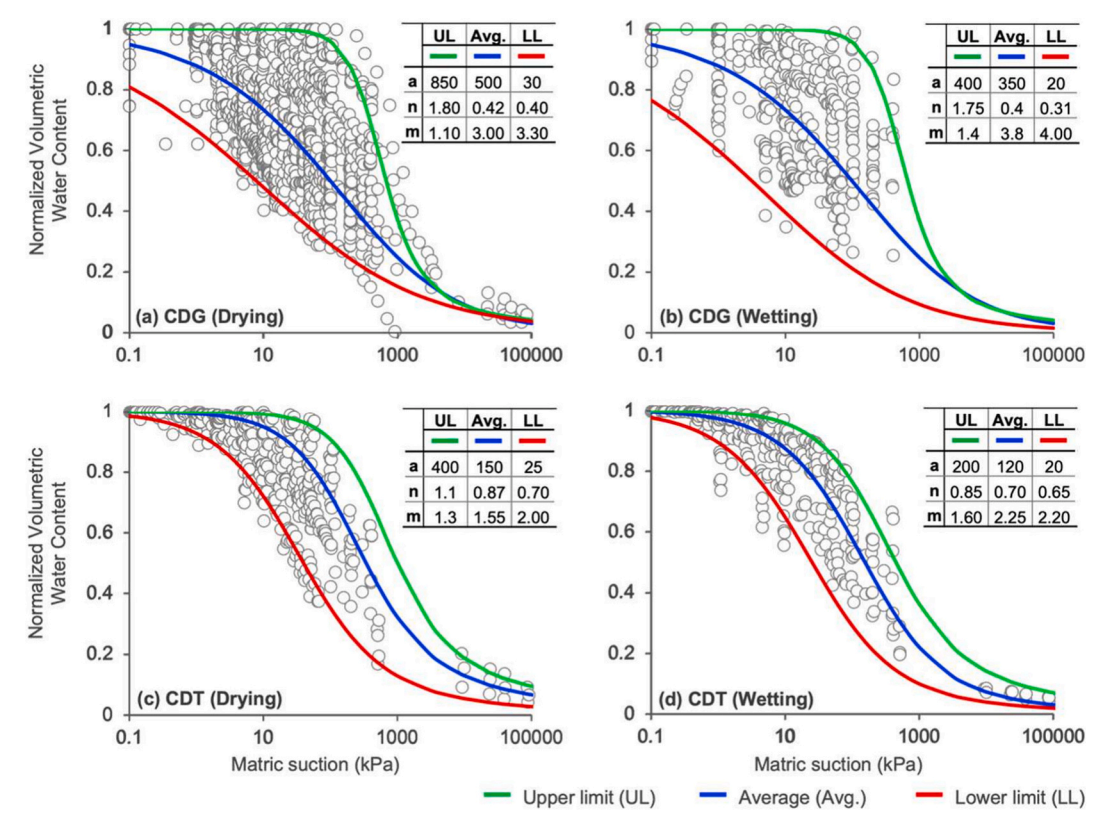


Fig. 13. SWCC envelope for typical Hong Kong soils: Completely Decomposed Granite (CDG) and Completely Decomposed Tuff (CDT)

kPa), rainfall intensity, and permeability. It should be noted, however, that in situations of relatively lower rainfall intensity ($q=0.5k_{\rm s}$ and $q=k_{\rm s}$) and higher initial suction (80–100 kPa, and even hydrostatic values), selecting SWCC with lower parameter a, resembling the wetting curve, offers conservative results. Moreover, caution is necessary when considering prolonged periods without rainfall as this could lead to a significant recovery of factor of safety, implying the potential importance of rainfall patterns, as shown in Fig. 8. Thus, it is important to consider the interplay between magnitude of suction, rainfall intensity, and rainfall pattern when selecting the appropriate SWCC to ensure a conservative design. Most recently, Natalia and Yang (2024) presented an interesting case study to elucidate the complicated role of the antecedent rainfall pattern in landslides in Hong Kong.

In this study, the strength and permeability of the unsaturated soil are estimated using the SWCC, shear strength, and saturated permeability parameters. Thus, it can reasonably quantify how different shapes of SWCC influence the stability analyses. Previous studies have observed the influence of the SWCC hysteresis on permeability (Fredlund et al., 1994; Kristo et al., 2019; Leung, 2011) and strength (Khoury and Miller, 2012; Vanapalli et al., 1996) parameters. Thus, it would be interesting to explore the influence of hysteresis on slope stability analysis in the future with consideration of these soil parameters. Additionally, as shown in Fig. 2, the issues related to the SWCC selection are not only caused by hysteresis but also variability. Studies have observed the relationship between particle size distribution and density, which commonly varies in the site with the shape of SWCC (Chai and Khaimook, 2020; Chin et al., 2010). The understanding related to the influence of the SWCC shape on slope stability analysis obtained from this study can be potentially extended and used for decision-making related to the variability.

6. Conclusions

The hysteresis phenomenon causes the soil under the same suction

level to have different volumetric water content, depending on the process the soil is experiencing, whether it is adsorption or desorption. Existing studies contained diverging views on the impact of hysteresis – whether the drying or wetting SWCC – should be adopted in rainfall-induced slope stability. This paper presents a comprehensive study through a literature review and a specifically designed parametric analysis to investigate the role of the hysteretic nature of SWCC in various scenarios of rainfall-induced slope failures, including differences in rainfall intensity, soil permeability, magnitude of initial suction. The importance of rainfall pattern is also taken into account. Furthermore, preliminary upper, average, and lower limit envelopes are proposed for the drying and wetting SWCC based on the collected measurements of typical soils in Hong Kong. These findings shed new light on the understanding of the diverging views in the literature, as detailed in the following:

- 1. The shape of the SWCC influences the slope stability analysis against rainfall. When SWCC with higher air-entry values are selected to represent the soil, the slope will have a lower minimum safety factor and more significant fluctuation in terms of safety factor against rainfall and no-rainfall period. Similar behavior can also be observed for SWCC with a steeper gradient or lower saturated volumetric water content θ_s . Generally, the drying curves tend to have higher air-entry values and steeper gradients. Likewise, the wetting curves have lower saturated volumetric water content θ_s .
- 2. Our study found a possible explanation for the diverging view of whether to adopt the drying or wetting SWCC to obtain a more conservative analysis. The relative relationship of the maximum initial suction used in the numerical analysis and the air-entry value of the SWCC influence the resulting conservative case, whether it is the drying or wetting curve. When the selected maximum initial suction is closer to the air-entry value, the slope with parameters resembling the drying curve or higher parameter a will give a more conservative analysis. Likewise, when the selected initial suction is

- closer to the residual zone, the SWCC with parameters resembling the wetting curve tends to give more conservative results.
- 3. The design conservativeness needs to be carefully defined, whether it is input parameters that give the lowest safety factor or those that give more conservative overall performance results. Some SWCC parameters result in the most critical safety factors but significantly fluctuate when evaluated against rainfall patterns that include low-intensity or no-rainfall periods. The reliability of the parameters needs to be examined when used.

CRediT authorship contribution statement

Levinna Natalia: Writing – original draft, Investigation, Formal analysis, Conceptualization. **Jun Yang:** Writing – review & editing, Supervision, Methodology, Funding acquisition, Conceptualization.

Declaration of competing interest

The authors declare that they have no known competing financial interests or personal relationships that could have appeared to influence the work reported in this paper.

Acknowledgements

The financial support provided by the Research Grants Council of Hong Kong through the GRF Grant No. 17207923 and the Hong Kong PhD Fellowship Scheme (HKPFS) is gratefully acknowledged.

Data availability

All data supporting the findings in this article are available from the corresponding author upon reasonable request.

References

- Anderson, S.A., Sitar, N., 1995. Analysis of rainfall-induced debris flows. J. Geotech. Eng. 121, 544–552. https://doi.org/10.1061/(asce)0733-9410(1995)121:7(544).
- Chai, J., Khaimook, P., 2020. Prediction of soil-water characteristic curves using basic soil properties. Transp. Geotech. 22, 100295. https://doi.org/10.1016/j. trgeo.2019.100295.
- Chen, Y., Yang, J., 2024. Initiation of flow liquefaction in granular soil slopes: drained versus undrained conditions. Acta Geotech. 19, 39–53. https://doi.org/10.1007/ s11440-023-01958-6
- Chin, K.-B., Leong, E.-C., Rahardjo, H., 2010. A simplified method to estimate the soil-water characteristic curve. Can. Geotech. J. 47, 1382–1400. https://doi.org/ 10.1139/t10-033
- Ebel, B.A., Loague, K., Borja, R.I., 2010. The impacts of hysteresis on variably saturated hydrologic response and slope failure. Environ. Earth Sci. 61, 1215–1225. https:// doi.org/10.1007/s12665-009-0445-2.
- Ering, P., Babu, G.L.S., 2016. Probabilistic back analysis of rainfall induced landslide- a case study of Malin landslide, India. Eng. Geol. 208, 154–164. https://doi.org/ 10.1016/j.enggeo.2016.05.002.
- Fredlund, D.G., 2015. Relationship between the laboratory SWCC and field stress state. In: Unsaturated Soil Mechanics - from Theory to Practice. Presented at the 6th Asia Pacific Conference on Unsaturated Soils (Guilin, China, 23–26 October 2015), Guilin, China. https://doi.org/10.1201/b19248.
- Fredlund, D.G., Xing, A., 1994. Equations for the soil-water characteristic curve. Can. Geotech. J. 31, 521–532. https://doi.org/10.1139/t94-061.
- Fredlund, D.G., Xing, A., Huang, S., 1994. Predicting the permeability function for unsaturated soils using the soil-water characteristic curve. Can. Geotech. J. 31, 533–546. https://doi.org/10.1139/t94-062.
- Freeze, R.A., 1969. The mechanism of natural ground-water recharge and discharge: 1. One-dimensional, vertical, unsteady, unsaturated flow above a recharging or discharging ground-water flow system. Water Resour. Res. 5, 153–171. https://doi.org/10.1029/wr005i001p00153.
- Gallage, C.P.K., Uchimura, T., 2010. Effects of dry density and grain size distribution on soil-water characteristic curves of sandy soils. Soils Found. 50, 161–172. https://doi. org/10.3208/sandf.50.161.
- Gan, J.K., Fredlund, D.G., 1995. Direct shear testing of a Hong Kong soil under various applied matric suctions. In: GEO Report No. 11.
- GeoSlope, 2018. Stability Modeling with GeoStudio. Calgary, Canada.
- Hillel, D., 2003. Introduction to Environmental Soil Physics. Part III: Liq. Phase, 127–148. https://doi.org/10.1016/b978-012348655-4/50008-3.
- Ho, K., Lacasse, S., Picarelli, L. (Eds.), 2016. Slope Safety Preparedness for Impact of Climate Change. CRC Press, London. https://doi.org/10.1201/9781315387789.

- Khoury, C.N., Miller, G.A., 2012. Influence of hydraulic hysteresis on the shear strength of unsaturated soils and interfaces. Geotech. Test. J. 35, 135–149. https://doi.org/ 10.1520/gtj103616.
- Kim, J., Hwang, W., Kim, Y., 2018. Effects of hysteresis on hydro-mechanical behavior of unsaturated soil. Eng. Geol. 245, 1–9. https://doi.org/10.1016/j. enggeo.2018.08.004.
- Kim, H., Lee, J.-H., Park, H.-J., Heo, J.-H., 2021. Assessment of temporal probability for rainfall-induced landslides based on nonstationary extreme value analysis. Eng. Geol. 294, 106372. https://doi.org/10.1016/j.enggeo.2021.106372.
- Ko, F.W.Y., Lo, F.L.C., 2016. Rainfall-based landslide susceptibility analysis for natural terrain in Hong Kong - a direct stock-taking approach. Eng. Geol. 215, 95–107. https://doi.org/10.1016/j.enggeo.2016.11.001.
- Kristo, C., Rahardjo, H., Satyanaga, A., 2019. Effect of hysteresis on the stability of residual soil slope. Int. Soil Water Conserv. Res. 7, 226–238. https://doi.org/ 10.1016/j.iswgr.2019.05.003
- Leong, E.C., Rahardjo, H., 1997. Review of soil-water characteristic curve equations. J. Geotech. Geoenviron. Eng. 123, 1106–1117. https://doi.org/10.1061/(asce)1090-0241(1997)123:12(1106).
- Leung, A.K., 2011. Field and Laboratory Studies of a Saprolitic Hillslope Subjected to Seasonal Variations. PhD Thesis,. Hong Kong University of Science and Technology.
- Li, A., 2003. Field Monitoring of a Saprolite Cut Slope. PhD Thesis,. The University of Hong Kong.
- Li, Y., Vanapalli, S.K., 2022. Models for predicting the soil-water characteristic curves for coarse and fine-grained soils. J. Hydrol. 612, 128248. https://doi.org/10.1016/j. ibvdrol.2022.128248
- Li, W.C., Lee, L.M., Cai, H., Li, H.J., Dai, F.C., Wang, M.L., 2013. Combined roles of saturated permeability and rainfall characteristics on surficial failure of homogeneous soil slope. Eng. Geol. 153, 105–113. https://doi.org/10.1016/j. enggeo.2012.11.017.
- Liu, X., Wang, Y., Li, D.-Q., 2020. Numerical simulation of the 1995 rainfall-induced Fei Tsui Road landslide in Hong Kong: new insights from hydro-mechanically coupled material point method. Landslides 17, 2755–2775. https://doi.org/10.1007/s10346-020-01442-2.
- Natalia, L., Yang, J., 2022. Investigation of rainfall-induced slope failures from an integrated perspective. In: Cloutier, C., Turmel, D., Maghoul, P., Locat, A. (Eds.), 8th Canadian Conference on Geotechnique and Natural Hazards. Presented at the 8th Canadian Conference on Geotechnique and Natural Hazards: Innovative geoscience for tomorrow, pp. 457–463.
- Natalia, L., Yang, J., 2024. New insights into the catastrophic slope failures at Sau Mau Ping: the role of antecedent rainfall pattern. Landslides 21, 1501–1514. https://doi.org/10.1007/s10346-024-02247-3.
- Ng, C.W.W., Wong, H.N., Tse, Y.M., Pappin, J.W., Sun, H.W., Millis, S.W., Leung, A.K., 2011. A field study of stress-dependent soil–water characteristic curves and permeability of a saprolitic slope in Hong Kong. Géotechnique 61, 511–521. https:// doi.org/10.1680/geot.8.p.157.
- Ni, J., 2017. Effects of Planting Spacing and Mixed Plant Types on Root Characteristics and Soil Suction. PhD Thesis., Hong Kong University of Science and Technology.
- Pang, Y.W., 1999. Investigation on Soil-Water Characteristics and their Applications on Stability of Unsaturated Soil Slopes. PhD Thesis,. Hong Kong University of Science and Technology.
- Pham, Q.H., 2001. An Engineering Model of Hysteresis for Soil–Water Characteristic Curves. MSc thesis., University of Saskatchewan, Canada.
- Pham, H.Q., Fredlund, D.G., Barbour, S.L., 2005. A study of hysteresis models for soil-water characteristic curves. Can. Geotech. J. 42, 1548–1568. https://doi.org/ 10.1139/t05-071
- Rianna, G., Pagano, L., Urciuoli, G., 2014. Rainfall patterns triggering shallow flowslides in pyroclastic soils. Eng. Geol. 174, 22–35. https://doi.org/10.1016/j. engeo.2014.03.004.
- Springman, S.M., Thielen, A., Kienzler, P., Friedel, S., 2013. A long-term field study for the investigation of rainfall-induced landslides. Géotechnique 63, 1177–1193. https://doi.org/10.1680/geot.11.p.142.
- Tami, D., Rahardjo, H., Leong, E.-C., 2004. Effects of hysteresis on steady-state infiltration in unsaturated slopes. J. Geotech. Geoenviron. Eng. 130, 956–967. https://doi.org/10.1061/(asce)1090-0241(2004)130:9(956).
- Torres, R., Dietrich, W.E., Montgomery, D.R., Anderson, S.P., Loague, K., 1998. Unsaturated zone processes and the hydrologic response of a steep, unchanneled catchment. Water Resour. Res. 34, 1865–1879. https://doi.org/10.1029/98wr01140.
- Tsai, T.-L., 2011. Influences of soil water characteristic curve on rainfall-induced shallow landslides. Environ. Earth Sci. 64, 449–459. https://doi.org/10.1007/s12665-010-
- Tsaparas, I., Rahardjo, H., Toll, D.G., Leong, E.C., 2002. Controlling parameters for rainfall-induced landslides. Comput. Geotech. 29, 1–27. https://doi.org/10.1016/ s0266-352x(01)00019-2
- Vanapalli, S.K., Fredlund, D.G., Pufahl, D.E., Clifton, A.W., 1996. Model for the prediction of shear strength with respect to soil suction. Can. Geotech. J. 33, 379–392. https://doi.org/10.1139/t96-060.
- Wang, G., Sassa, K., 2003. Pore-pressure generation and movement of rainfall-induced landslides: effects of grain size and fine-particle content. Eng. Geol. 69, 109–125. https://doi.org/10.1016/s0013-7952(02)00268-5.
- Wong, H.N., Ho, K.K.S., 1993. Systematic investigation of landslides caused by a severe rainstorm in Hong Kong. HKIE Trans. 3, 17–27. https://doi.org/10.1080/ 1023697x.1996.10667704.
- Yang, H., Rahardjo, H., Leong, E.-C., Fredlund, D.G., 2004. Factors affecting drying and wetting soil-water characteristic curves of sandy soils. Can. Geotech. J. 41, 908–920. https://doi.org/10.1139/t04-042.

- Yang, H.-Q., Zhang, L., Gao, L., Phoon, K.-K., Wei, X., 2022. On the importance of landslide management: Insights from a 32-year database of landslide consequences and rainfall in Hong Kong. Eng. Geol. 299, 106578. https://doi.org/10.1016/j. engep. 2022.106578.
- Yang, J., Wei, L.M., 2012. Collapse of loose sand with the addition of fines: the role of particle shape. Géotechnique 62 (12), 1111–1125. https://doi.org/10.1680/geot.11.
- Yang, Y.-S., Yeh, H.-F., Ke, C.-C., Wei, L.-W., 2024. Assessing shallow slope stability using electrical conductivity data and soil hydraulic characteristics. Eng. Geol. 331, 107447. https://doi.org/10.1016/j.enggeo.2024.107447.
- Zhai, Q., Rahardjo, H., Satyanaga, A., 2016. Effects of variability of unsaturated hydraulic properties on stability of residual soil slopes. In: Unsaturated Soil Mechanics - from Theory to Practice. Presented at the 6th Asia Pacific Conference on Unsaturated Soils (Guilin, China, 23–26 October 2015), Guilin, China. https://doi. org/10.1201/b19248.
- Zhai, Q., Rahardjo, H., Satyanaga, A., Dai, G., Du, Y., 2020. Estimation of the wetting scanning curves for sandy soils. Eng. Geol. 272, 105635. https://doi.org/10.1016/j. enggeo.2020.105635.
- Zhang, L.L., 2007. Effects of soil hydraulic hysteresis on slope reliability. In: Huang, H., Zhang, L. (Eds.), ISGSR 2007 First International Symposium on Geotechnical Safety and Risk. Shanghai, China.
- Zhang, L.L., Li, J., Li, X., Zhang, J., Zhu, H., 2016. Rainfall-Induced Soil Slope Failure Stability Analysis and Probabilistic Assessment. CRC Press, Boca Raton. https://doi. org/10.1201/b20116-11.
- Zhang, L., Tang, X., Yang, J., 2023. Rainfall-induced flowslides of granular soil slopes: insights from grain-scale modeling. Eng. Geol. 323, 107223. https://doi.org/10.1016/j.enggeo.2023.107223.
- Zou, X., Li, D., Wang, S., Gu, S., Wu, W., 2024. Instability and deformation behaviors of root-reinforced soil under constant shear stress path. Eng. Geol. 343, 107762. https://doi.org/10.1016/j.enggeo.2024.107762.